NIH Public Access
Author Manuscript
Insect Biochem Mol Biol. Author manuscript; available in PMC 2014 April 01.

Published in final edited form as:
Insect Biochem Mol Biol. 2013 April ; 43(4): 376–387. doi:10.1016/j.ibmb.2013.01.002.

Receptors for the Neuropeptides, Myoinhibitory Peptide and SIFamide, in Control of the Salivary Glands of the Blacklegged Tick *Ixodes scapularis*

Ladislav Šimo, **Juraj Koči**, and **Yoonseong Park**
Department of Entomology, Kansas State University, Manhattan, KS 66506-4004, USA

Abstract

Tick salivary glands are important organs that enable the hematophagous feeding of the tick. We previously described the innervation of the salivary gland acini types II and III by a pair of protocerebral salivary gland neurons that produce both myoinhibitory peptide (MIP) and SIFamide (Šimo et al., 2009b). In this study we identified authentic receptors expressed in the salivary glands for these neuropeptides. Homology-based searches for these receptors in the *Ixodes scapularis* genome sequence were followed by gene cloning and functional expression of the receptors. Both receptors were activated by low nanomolar concentrations of their respective ligands. The temporal expression patterns of the two ligands and their respective receptors suggest that the SIFamide signaling system pre-exists in unfed salivary glands, while the MIP system is activated upon initiation of feeding. Immunoreactivity for the SIFamide receptor in the salivary gland was detected in acini types II and III, surrounding the acinar valve and extending to the basal region of the acinar lumen. The location of the SIFamide receptor in the salivary glands suggests three potential target cell types and their probable functions: myoepithelial cells that may function in the contraction of the acini and/or the control of the valve; large, basally located dopaminergic granular cells for regulation of paracrine dopamine; and neck cells that may be involved in the control of the acinar duct and its valve.

Keywords

MIP receptor; SIFamide receptor; GPCR functional assay; salivary glands; acini; synganglion

1. Introduction

A large number of G protein-coupled receptors (GPCRs) function as receptors for neuropeptides and protein hormones that control a vast majority of biological functions, such as reproduction, development, molting, behavior and feeding, in arthropods. In genomic and post-genomic analyses of many model arthropod species, deorphanization of neuropeptides and their receptors has led to the discovery of new peptidergic systems and functions. A combination of bioinformatics and advanced biotechnologies, such as peptidomic analyses and RNA interference (RNAi), has revealed more comprehensive lists

© 2013 Elsevier Ltd. All rights reserved.

Corresponding author: Yoonseong Park, ypark@ksu.edu.

Publisher's Disclaimer: This is a PDF file of an unedited manuscript that has been accepted for publication. As a service to our customers we are providing this early version of the manuscript. The manuscript will undergo copyediting, typesetting, and review of the resulting proof before it is published in its final citable form. Please note that during the production process errors may be discovered which could affect the content, and all legal disclaimers that apply to the journal pertain.

NIH-PA Author Manuscript
NIH-PA Author Manuscript
NIH-PA Author Manuscript

NIH-PA Author Manuscript

NIH-PA Author Manuscript

NIH-PA Author Manuscript

of neuropeptides and their receptors and facilitated the investigation of their biological roles and evolutionary processes.

The blacklegged tick, *Ixodes scapularis*, is a well-known vector of *Borrelia burgdorferi*, which causes Lyme disease. An analysis of the *I. scapularis* genome (Hill and Wikel, 2005) has provided opportunities for the exploration of the biology of neuropeptides and their receptors in this unique hematophagous arthropod. A female tick must feed on a host for at least one week to achieve full engorgement. During feeding, the tick's body weight increases approximately 100-fold. The salivary secretion of the tick mediates pathogen transmission and promotes successful feeding by suppressing and modulating the host's immune system (Bowman et al., 1997; Bowman and Sauer, 2004; Ribeiro et al., 2006). In addition, salivary secretion facilitates the excretion of excessive water and waste during feeding (Kaufman and Phillips, 1973a; 1973b; Sauer and Hair, 1971).

The mechanisms involved in the control of tick salivary secretion have long been under study because a better understanding of these mechanisms could lead to the development of tools to disrupt the saliva secretory process. Previous pharmacological studies suggested that pilocarpine, a muscarinic acetylcholine receptor agonist, activates the synganglion, the central nervous system of the tick, which generates the neural signals that lead to salivary secretion (Kaufman, 1978; McSwain et al., 1992). Dopamine, which is produced in the salivary glands (SGs), acts as a paracrine factor for the activation of SG acini for fluid secretion (Kaufman et al., 1999; Šimo et al., 2011a).

Tick SGs are a large pair of grape-like clusters that are located anterolaterally on the ventral part of the body cavity. Female tick SGs consist of three types of acini (I, II and III). Agranular acini type I are attached mainly to the anterior main salivary duct, while both granular acini types II and III are located more posteriorly and are attached to the main salivary duct and its branches. The type II and III acini, which are considered to be primarily involved in the production of bioactive components and the excretion of excess water and ions, respectively, are composed of several different cell types (Binnington, 1978). Given that there are a number of different bioactive salivary components that are produced and secreted from various cells in the different acini of the SGs at different feeding phases, tick salivation is likely orchestrated by a complex combination of neural and hormonal mechanisms.

The tick synganglion contains multiple neuronal cells of various sizes and shapes, which form a neuronal cortex on the surface of segmented lobes (Sonenshine, 1991). Aminergic and peptidergic neuronal cells were characterized by immunohistochemistry (IHC) (Hummel et al., 2007; Šimo et al., 2009a; 2009b; 2011b). Our previous study utilized 15 different antibodies, which were originally raised against neuropeptides in many different species of insects and crustaceans, and found that the synganglion was rich in neuropeptides (Šimo et al., 2009a); these findings were confirmed by a peptidomic analysis (Neupert et al., 2009), as well as an analysis of homology-based neuropeptide gene prediction (Christie, 2008; Šimo and Park, unpublished data).

Šimo et al. (2009b) previously described a pair of protocerebral SG (PcSG) neurons with axonal projections that innervate the basal regions of the SG acini types II and III. The PcSG neurons and their projections contain both myoinhibitory peptide (MIP) and SIFamide, which were confirmed by matrix-assisted laser desorption/ionization (MALDI) analyses, *in situ* hybridization, and immunohistochemistry. In the present study, we identified and functionally characterized the receptors for MIP and SIFamide in the SGs of the blacklegged tick, *I. scapularis*. The temporal and spatial expression patterns of both ligands and their receptors were investigated using antibodies and quantitative PCR. This study highlights the

NIH-PA Author Manuscript

NIH-PA Author Manuscript

NIH-PA Author Manuscript

unique neural control of tick SGs and suggests possible functions of the neuropeptidergic systems in tick salivary secretion.

2. Material and methods

2.1 Animals and tick feeding

Unfed adult *I. scapularis* ticks were obtained from a tick-rearing facility at Oklahoma State University. Approximately 30 individuals of *I. scapularis*, both male and female, were kept in a polypropylene tube (9 × 2.5 cm) with a small piece of filter paper (4 × 1 cm) in the vial. The tubes were kept in a dark, humid chamber at 4 °C. T ick feeding was performed on New Zealand White rabbits (Myrtle's Rabbitry, TN). Female and male ticks were placed at a 1:1 ratio in the feeding chamber that was attached to the back of a rabbit. Rabbits were cared for in accordance with the guidelines set by the Institutional Animal Care and Use Protocol (IACUC Approval No. 3050) of Kansas State University.

2.2 Gene cloning and sequence analyses

Blast searches of the *I. scapularis* genome (http://www.vectorbase.org) yielded two genes, *mip-r1* and *mip-r2*, encoding putative *I. scapularis* MIP receptors (MIP-R), and a single gene, *sifa-r*, encoding a putative SIFamide receptor (SIFa-R). The query sequences were based on previous reports of the *Drosophila melanogaster* MIP-R (also known as sex peptide receptor; AAF46037.2) (Yapici et al., 2008) and SIFa-R (AAN13859.2) (Jorgensen et al., 2006). The predicted full-length open reading frames (ORF) of *mip-r1* and *sifa-r* were amplified from cDNA, which was isolated from whole bodies of partially fed, mixed-stage females, by polymerase chain reaction (PCR) using the primers listed in Table 1. The PCR products for *mip-r1* and *sifa-r* were cloned into the pcDNA3.1D/V5-His-TOPO (Invitrogen, Carlsbad, CA) and pGEM-T-easy vectors (Promega, Madison, WI) and then sequenced. To determine the 5' end of the ORF of *mip-r2*, we performed a rapid amplification of cDNA ends (RACE) reaction followed by PCR using primers for various regions of the 5' end of the genomic sequence.

For the phylogenetic analyses, putative translations were aligned using the CLUSTAL program (Thompson et al., 1994). Only the sequences of conserved regions, including the transmembrane domains 1–7, were used for the construction of a neighbor-joining tree with 500 bootstrap resamplings using the MEGA5 software (Kumar et al., 2008). Transmembrane segments were predicted using the HMMTOP Server v2.0 software (http://www.enzim.hu/hmmtop/) (Tusnady and Simon, 1998).

2.3 Receptor functional assays

The full-length ORFs of *mip-r1* and *sifa-r* were inserted into the pcDNA3.1D/V5-His-TOPO (Invitrogen) and pcDNA3.1(+) (Invitrogen) plasmids, respectively. Transient expression of *mip-r1* and *sifa-r* with the aequorin reporter (human cytoplasmic aequorin, (Vernon and Printen, 2002) in Chinese hamster ovary (CHO) cells was used for detection of increased luminescence as the reporter for ligand-induced calcium mobilization. For the MIP-R1 assay, CHO cells were co-transfected with the G protein subunit Gα16, which is known to provide a promiscuous link to the calcium mobilization signaling pathway (Park et al., 2002; Park et al., 2003).

Luminescence assays were performed in opaque 96-well microplates (Corning) using an Orion microplate luminometer (Berthold Detection Systems). The following peptides were chemically synthesized with >80% purity based on MALDI and HPLC analyses (Bio Basic Inc., Canada): MIP1 (GGDWNALSGMWamide), MIP2 (ASDWNRLSGMWamide), MIP3 (ENHWNDLSGYWamide), and SIFamide (AYRKPPFNGSIFamide). The negative control

NIH-PA Author Manuscript

NIH-PA Author Manuscript

NIH-PA Author Manuscript

consisted of cells transfected with the reporter construct aequorin only, which did not show any response to the ligands tested. A different negative control consisted of transfected cells that were treated with various other neuropeptides (10 μM concentration) such as: *D. melanogaster* ecdysis triggering hormone 2 (ETH2), *Rattus* arginine vasopressin peptide (AVP), *Tribolium*. *castaneum* arginine vasopressin peptide like (AVPL), *D. melanogaster* corazonin and FMRFamide, *D. melanogaster* crustacean cardioactive peptide (CCAP), *Tenebrio molitor* diuretic hormone (DH37), *I. scapularis* SIFamide (only for the MIP-R1 assay) and *I. scapularis* MIP2 (only for the SIFa-R assay).

2.4 Quantitative real-time reverse transcriptase-PCR (qRT-PCR)

Female ticks were washed with 70% ethanol, rinsed in distilled water, and dissected in ice-cold sterile phosphate buffered saline (PBS; 137 mM NaCl, 1.45 mM NaH2PO4, 20.5 mM Na2HPO4, pH 7.2). Dissected organs were immediately frozen in tubes placed on dry ice and stored at −80 °C for later use. Salivary glands (SG s) and synganglia were dissected from ticks that were unfed, partially fed for 1–6 days or repleted (i.e., fed for 7–9 days). For tissue-specific qRT-PCR analyses, cDNAs from all different stages were pooled to ensure the detection of temporally fluctuating message in each tissue. Total RNA was extracted using either Trizol reagent (Invitrogen) followed by a Turbo DNAse treatment (Ambion) or the RNeasy Plus Micro Kit (Qiagen), which utilizes an on-column DNase treatment to obtain DNA-free RNA.. Reverse transcription according to the manufacturer's oligo(dT)20-based protocol was followed by real-time PCR using SYBR premix Ex Taq (Takara Bio). All data presented are for at least three biological replicates unless otherwise specified in the figure captions.

Primers for the qRT-PCR assay (Table 1) amplified a 233 bp-long fragment for mip-r1, a 248 bp-long fragment for the ligand *mip*, a 152 bp-long fragment for *sif-r*, and a 154 bp-long product for the ligand *sifamide*. The 80 bp-long amplicon encoding ribosomal protein S4 (Accession No. DQ066214) served as a reference gene as described in previous studies (Koči et al., 2012; Šimo et al., 2009b). Because of the high nucleotide sequence identity (69.7%) between *mip-r1* and *mip-r2* in the conserved region assembled by the blast algorithm BLOSUM 60, the qRT-PCR amplicon for *mip-r1* was verified by sequencing to confirm the specificity. The amplicons in the qRT-PCR were verified by melting curves and electrophoresis on a 1.5% agarose gel to ensure both the absence of primer-dimer formations and the specificity of the amplicons. Mean Ct values for the reference and target genes were generated from technical duplicates and used to calculate ΔΔCt values (Livak and Schmittgen, 2001). Fold-differences in the expression of target genes in tissue-specific and stage-specific sample sets were deduced from a calibrated sample assigned with the value of 1. Statistics on the mean ± SD were performed on at least three biological replicates using a one-way Student t-test ($P \leq 0.05$) and Origin v7 software.

2.5 Antibodies and immunohistochemistry

The antibodies for the MIP and SIFamide neuropeptides have been previously described (Šimo et al., 2009b). Both antibodies recognized only neuronal cell bodies and their projections in the *I. scapularis* synganglion. Representative cells stained by the antibodies generally coincided with *in situ* hybridization staining for their respective mRNAs (Šimo et al., 2009b).

Affinity purified antibodies against MIP-R1 and SIFa-R were raised in chickens (Genescript, New Jersey). An antigenic peptide for each receptor was designed for the region that was predicted to have a high surface probability and antigenicity and a low probability of post-translational modification. The 20 carboxy-terminal amino acid residues for MIP-R1 (CSSRYSLVNGPRTVTNETVL) and SIFa-R

NIH-PA Author Manuscript

NIH-PA Author Manuscript

NIH-PA Author Manuscript

(CTRGLSRYDTQCEYLSTSAV) were chemically synthesized and conjugated to keyhole limpet hemocyanin using the cysteines at the N-termini of each of the epitopes. The final bleed was used for affinity purification. The respective chicken pre-immune sera for each antibody were used as negative controls (Supplementary Fig. S1 A and B). The specificity of each antibody was characterized by detecting positive signals in Chinese hamster ovary (CHO) cells transfected with *mip-r1* or *sifa-r* (Supplementary Fig. S1 C–E).

For whole-mount immunohistochemical staining of tick synganglia and SGs, we followed a procedure that was previously established (Šimo et al., 2009a; 2009b). Samples fixed in Bouin's solution were washed in PBS containing 1% Triton X-100 (PBST). For receptor staining, SGs were treated with 10 μg/ml proteinase K (New England BioLabs) for 10 minutes for epitope retrieval, washed three times with PBST,,pre-adsorbed with 5% normal goat serum (Sigma, St. Louis, MO), and subsequently incubated with the appropriate antibody or a mixture of antibodies. Dilutions for all primary antibodies were 1:1000. The secondary antibodies used in the study were : Alexa 594 or 488-goat anti-rabbit IgG, Alexa 594 or 488- goat anti-mouse IgG and Alexa 594 or 488-goat anti-chicken IgG (Molecular Probes, Carlsbad, CA). For the immunohistochemical staining of sectioned SGs, we used standard paraffin embedding protocol for ~10 μm-thick sections with an additional step for epitope retrieval, in which the slides were steamed (Black and Decker) for 35 minutes in epitope retrieval solution (IHC-Tek, IHCWorld) before incubation with primary antibody. Images were acquired using a confocal microscope (Zeiss 510 Meta or LSM 700). Image enhancements (i.e., alterations in contrast and brightness) were performed in Adobe Photoshop 7.0.

2.6 The nomenclature of peptidergic neurons

For the naming of peptidergic neurons, we followed a nomenclature system previously used for the hard tick R. appendiculatus (Šimo et al., 2009a). The first two letters of each name refer to the position of each neuron in a specific lobe of the synganglion, specifically cheliceral (Ch), prothocerebral (Pc), pedal 1–4 ($Pd_{1–4}$), opisthosomal (Os), or postesophageal (Po). The letters that follow the first two letters of each name refer to the anatomical location of the neuron, specifically dorsal (D), ventral (V), anterior (A), posterior (P), medial (M) or lateral (L). Neurons that innervate the acini of the salivary glands were labeled as SG.

3. Results

3.1 The genes encoding the MIP and SIFamide receptors

Blast searches for MIP and SIFamide receptors in the *I. scapularis* genome yielded two putative MIP receptors with highly conserved regions (*mip-r1* and *mip-r2*) and one putative *sifa-r* (Fig. 1A–D). The sequences were further analyzed for predictions of gene structures and for primer designs. We obtained the full-length ORFs for *mip-r1* and *sifa-r*, while *mip-r2* lacked a 5' translation initiation site. All receptor sequences in this study contained typical motifs for seven-transmembrane α-helical proteins (Fig. 1C,D).

Phylogenetic analyses with the MIP-R of multiple species of insects and the sex peptide receptor of *D. melanogaster* suggested an orthologous cluster containing *I. scapularis* MIP-R1 and MIP-R2 and other MIP-Rs (Fig. 1A). The intronless open reading frame (ORF) of *mip-r1* is 1155 bp, and the putative *mip-r2* ORF is longer than 1110 bp (Fig. 1E). *Mip-r1* and *mip-r2* are located back-to-back in the same contig (DS814451), based on *I. scapularis* genomic data (Fig. 1E), and exhibit a 71.3% amino acid sequence identity to each other. Since we were unable to identify the 5' translation initiation site of *mip-r2*, we examined the genomic sequence of the 5' region of *mip-r2* and compared it to the assembled genomic

NIH-PA Author Manuscript

NIH-PA Author Manuscript

NIH-PA Author Manuscript

sequence in the database. We found two nucleotide insertions, a thymidine (T) and a cytosine (C), which restored the reading frame for the putative translation similar to the corresponding region of *mip-r1* (Fig. 1E and Supplementary Fig. S2); however, there is still the ambiguity of the 5' ORF of *mip-r2*. Further efforts to identify the 5' end of the gene using 5' rapid amplification of cDNA ends (RACE) and RT-PCR using primers designed on various 5' upstream sequences were not successful in finding the 5' end start codon of the *mip-r2* ORF.

We examined whether the incomplete ORF of *mip-r2* was transcribed. Various pairs of PCR primers did not provide a conclusive result (Supplementary Fig. S2). Although we obtained faint bands of expected sizes from certain primer sets in RT-PCR analyses, using salivary gland cDNA from a DNase treated template, we could not exclude the possibility that the faint gel bands were generated from the amplification of genomic DNA, because *mip-r2* is an intronless gene. We also examined the possible occurrence of alternatively spliced forms of the transcript, producing mRNAs spanning both genes, *mip-r2* and *mip-r1*, by using primer sets with one primer in each gene (Supplementary Fig. S2). None of these primer sets produced an amplicon, which indicates that *mip-r1* and *mip-r2* are independent genes.

The *I. scapularis sifa-r* ORF consists of 1203 bp (Fig. 1F) and is composed of three exons (379 bp, 100 bp and 724 bp) that are interrupted by two introns (~113,780 bp and 2141 bp; Fig. 1F). Phylogenetic analyses of the *I. scapularis* SIFa-R and SIFa-Rs of other arthropod species demonstrated a clear orthologous cluster, consisting of the *I. scapularis* SIFa-R and other SIFa-Rs (Fig. 1B). The GenBank Accession Numbers of the sequences used for these phylogenetic analyses are listed in the Fig. 1 caption.

3.2 Ligand–receptor interactions

Three putative mature MIPs, encoded by one gene in *I. scapularis* (Šimo et al., 2009b), were all highly active on the MIP-R1 receptor (Fig. 2A), with EC_{50} values of 40 nM, 32 nM, and 15 nM for MIP1, MIP2, and MIP3, respectively. MIP2 was the only ligand identified in the previous MALDI analysis (Šimo et al., 2009b). Robust luminescent responses were also generated when SIFa-R was heterologously expressed; in this case, an EC_{50} value of 5.8 nM was observed in response to the SIFamide ligand (Fig. 2B). For all of the active doses of the SIFamide ligand in the SIFa-R assay, the increase in luminescence was observed immediately after the ligand was applied, and this luminescence peaked within the first 5 sec of ligand application. In contrast, all of the active doses of MIP ligands in the MIP-R1 assay elicited slower responses, with the luminescence peaking more than 10 sec after the treatments (Fig. 2C and D).

The ligands tested in this study showed no activity on cells that were not transfected with a receptor, indicating that the luminescent responses were specifically mediated by the transfected receptors. The cells that expressed MIP-R1 or SIFa-R were activated only by MIPs 1–3 and SIFamide, respectively, and did not react to any other tested ligands (see section 2.3 The receptor functional assays for the list of ligands tested).

3.3 The spatial and temporal levels of the *mip-r1* and *sifa-r* receptors in the salivary glands

The *mip-r1* and *sifa-r* transcripts were abundant in female SGs and synganglia from a mixed sample of unfed, 1^{st} – 6^{th} day fed, and replete females, while a low, but detectable level of *sifa-r* transcript was found in carcasses (Fig. 3).

Dynamic changes in the mRNA levels of the receptors in the SGs were observed. The *mip-r1* transcript was minimally detectable before feeding, increased after the initiation of feeding, peaked at day 4 (~20× higher than that of unfed), and continued to fluctuate thereafter (Fig. 4A). In contrast, unfed ticks already had *sifa-r* transcripts, and the onset of

NIH-PA Author Manuscript

NIH-PA Author Manuscript

NIH-PA Author Manuscript

feeding coincided with a mild reduction in the transcript expression level, followed by an increase at the end of feeding (Fig. 4A). The expression patterns of the receptor mRNAs in the SGs are similar to those of the corresponding mature peptide ligands that were measured by the frequency of positive immunohistochemical signal at the axon terminals reaching into the basal part of the acini (Fig. 4B and in next 3.4 section).

3.4 Immunohistochemistry of the MIP and SIFamide neuropeptides and their receptors in the salivary gland

The innervation of the SGs by a pair of PcSGs in the synganglion in unfed ticks was described in our earlier study (Šimo et al., 2009b). The current report expands upon that study by analyzing the entire feeding phase of the tick with a large number of samples. We investigated MIP- and SIFamide-immunoreactivity (IR) in the axon terminals located in the basal region of the acini; a total of 115 female ticks were used over the full course of a feeding phase in at least 3 different sets of biological replicates. Although acini types II and III increased markedly in size during feeding, specifically from ~40 μm up to ~150 μm in diameter, the MIP-and SIFamide-IR in the axon terminals remained associated with the basal regions of the acini. In acini type II, the IR in the axon terminals slightly increased in length from ~25 μm to ~50 μm during feeding, while the length of the axon terminals in acini type III remained constant at ~25 μm (Fig. 5). A low number of positive MIP-IR samples were found in specimens that were either unfed or fed for up to 2 days, while the frequency of positive samples significantly increased after the 2nd day of feeding (Fig. 4B). The SIFamide-IR in the axon terminals was 100% positive in all samples examined during the various feeding stages (Fig. 4B), although the relative strengths of the IR changed over the feeding duration (see Discussion for more details). The fully engorged females (i.e., 0–24 h after repletion) exhibited a 50% positive sample frequency for both MIP and SIFamide (Fig. 4B). All samples were doubly stained for both MIP and SIFamide.

SIFa-R-IR was examined in both whole-mount specimens and paraffin sections after an extensive optimization of the steps for epitope retrieval (see section 2.5 Antibody and immunohistochemistry). In acini type III, a strong IR was detected in the region surrounding the acinar duct and extending into the inner part of the acini on the luminal surface of the basal region of the acini (Fig. 6A–C). Double-staining for SIFa-R and its ligand, SIFamide, showed that the SIFa-R-IR on the luminal surface of the basal region (i.e., acini types II and III) is closely associated with the axon terminals that express SIFamide (Fig. 6D–F). In acini type II, the SIFa-R-IR was observed mainly in the basal region of the acini lumen (Fig. 6D), which is similar to the IR seen in acini type III (Fig. 6E). In addition, the IR of type II acini was occasionally dispersed more apically on the luminal surface of the acini, which corresponds with the longer projections of the PcSG axon terminals in the type II acini. Although the positive signal on the neck region is apparent, a clear conclusion for the IR in the central part of the acinar duct (empty arrow heads in Fig. 6C) is obscured because the cuticular structure of SG ducts is often autofluorescent (empty arrow heads in Fig. 6A and C). The SIFa-R-IR was observed in the SGs of unfed (data not shown), 4-, and 5-day-fed females (Fig. 6), indicating a constitutive presence of the SIFa-R.

In contrast, we were unable to obtain a positive signal for MIP-R1 in the SG, although we found a specific MIP-R1-IR pattern in the synganglia (Figs. 7 A and 8 A and A') and when the receptor was heterologously expressed in CHO cells (Supplementary Fig. S1 C).

3.5 MIP and SIFamide receptors and their ligands in the female synganglia

Positive MIP-R1-IR in the synganglia was observed in nineteen pairs of protocerebral neurons (PcAM, $PcDM_{1–4}$, $PcVM_{1–6}$, $PcVL_{1,2}$ and PcDM), four cheliceral neurons ($ChV_{1–4}$), eight pedal neurons ($Pd_1DL_{1,2}$, $Pd_1VL_{1,2}$, $Pd_{2–4}DM$, and Pd_4VM), and eight

NIH-PA Author Manuscript

NIH-PA Author Manuscript

NIH-PA Author Manuscript

opistosomal neurons ($OsDM_{1–3}$, OsVM, and $OsVM_{1,2}$). The IR was also observed in axonal projections within the synganglia, which arborized in the protocerebrum and all four pairs of the pedal lobes (Figs. 7A and 8A and A').

In addition to the previously described MIP-immunoreactive neurons in unfed *I. scapularis* females (Šimo et al., 2009b), we observed a strong IR in two pairs of protocerebral dorso-medial neurons ($PcDM_{1,2}$), one pair of giant neurons located in the postesophageal region (PoVM), and twelve pairs of segmental neurons in the pedal ganglia I–IV ($Pd_{1–4}VM_{1–12}$) in five-day-fed females.(Fig. 8B and B').

SIFa-R-IR was observed in ten pairs of protocerebral neurons ($PcAM_{1–3}$, PcVM, PcDM1–2, PcDL, and $PcVM_{1–3}$), four pairs of pedal neurons ($Pd_{1–4}VM$), and seven pairs of opistosomal neurons (OsDM, OsVM, $OsVM_{1–4}$, and $OsVM_5$; Figs. 7B and 8D and D'). A positive IR was also observed in the axonal projections within the synganglia, which arborized in all four pedal lobe pairs. Costaining with antibodies against SIFamide (Figs. 8E and E') and its receptor revealed that the SIFa-R-IR projections in the pedal lobes are closely associated with the SIFamide ligand IR (Fig. 8F'). The SIFamide projections are from the $PcMV_{1–4}$ neurons, and the SIFa-R-IR projections are likely from OsVM cells.

The transcripts for *mip-r1* and *mip* in the synganglia were constitutively present over the course of tick feeding, with a mild degree of fluctuation (i.e., within 3×) and trends of decreasing mRNA levels toward the end of the feeding, especially for *mip* (Fig. 9A). The transcripts for *sifa-r* and *sifamide* in the synganglia were also relatively stable over the course of tick feeding, except for a significant reduction (i.e., ~50% of unfed ticks) in both transcripts that occurred in the middle of the feeding period (3^{rd} day, Fig. 9B).

4. Discussion

Multiple approaches in this study revealed authentic receptors for MIP and SIFamide and led to functional implications. Homology-based identification of the genes, followed by studies of temporal and spatial expression patterns and functional characterization of the receptors, all together support the MIP and SIFamide signaling systems as important neural factors controlling the SGs in ticks.

In the receptor functional assays, the pattern of calcium elevation, as measured by the luminescence of the aequorin reporter (Park and Adams, 2010), indicated that SIFa-R is efficiently linked to the intracellular signaling pathway, leading to calcium mobilization. The robust and rapid calcium responses of SIFa-R-transfected cells indicate that calcium elevation is part of the endogenous SIF-R's downstream signaling pathway. On the other hand, the slow calcium elevation in the MIP-R1 activation by MIP ligands might indicate that the endogenous coupling of MIP-R is not through calcium elevation, although it is important to note that this assay system relies upon the efficiency of synthetic molecular interactions in a heterologous system.

Investigations of the temporal dynamics of the levels of ligands and their receptors over the feeding period indicated opposing temporal trends of the two different ligand-receptor pairs. The levels of *mip-r1* were lowest in unfed ticks and peaked in the later phases of feeding, while the trends for the levels of *sifa-r* were in an opposite pattern, high in unfed and lowest in the middle of the feeding period (Fig. 4A). The frequencies of ligand-IR in the SGs (Fig. 4B) partially coincided with the receptor expression patterns; low in unfed and gradually increasing over the feeding period for MIP-IR. Furthermore, we observed stronger intensities of SIFamide staining compared to that of MIP in the unfed and early feeding stages (1^{st} – 3^{rd} days) and an opposite pattern in the later feeding phases (4^{th} – 6^{th} days), although accurate quantitative comparisons were not possible after double-staining for MIP

NIH-PA Author Manuscript

NIH-PA Author Manuscript

NIH-PA Author Manuscript

and SIFamide. In conclusion, we speculate that the opposing temporal trends of the two different signaling systems, ligands for both of which originate from PcSG neurons and are delivered through the same axon terminals (Šimo et al., 2009b), may indicate a dynamic mechanism for the control of the SGs.

The immunohistochemistry of SIFa-R in this study, along with the ultrastructure of SG acini described in previous studies (Binnington, 1978; Coons et al., 1994; Coons and Roshdy, 1973; Fawcett et al., 1986; Krolak et al., 1982; Meredith and Kaufman, 1973; Roshdy and Coons, 1975), suggests that there are at least three different target cell types that exhibit different functions in the control of the SGs. Although previous descriptions of these cell types and the number of the basally located acini cells have varied depending on the tick species, feeding phases, and methods of investigation, three commonly described cell types were identified in the basal region of the acini, specifically myoepithelial cells, basal granular cells, and neck cells. The myoepithelial cell (Coons et al., 1994), also known as the Cap cell (Krolak et al., 1982; Meredith and Kaufman, 1973) or adluminal cell (Fawcett et al., 1986; Sauer et al., 1995), has narrow cellular branches lining the acini luminal surface and extends to the upper lip region of the acinar valve. The myoepithelial cell was proposed to function in the contraction of the acini (Coons et al., 1994; Coons and Roshdy, 1973), but also may function in the control of the acinar valve. Both functions are important for controlling expulsion of the luminal contents into the SG duct. Alternatively, the neuropeptidergic systems may be involved in the control of the synthesis and/or secretion of paracrine dopamine in large basal granular cells (Šimo et al., 2011a). This possibility is supported by the presence of dopamine-immunoreactive granules (Šimo et al., 2011a) in the basal cells (a- and d- cells in type II and III acini, respectively) (Binnington, 1978). Finally, a third possible target cell type is the neck cell that lines the acinar duct. This cell likely functions in the control of the valve. One or more proposed functions for MIP and SIFamide involve type II and III acini, which both contain these three types of cells with minor differences in the anatomical details.

MIP-R immunostaining in the SGs was not observed, although the same antibody did reveal specific staining patterns for the synganglion and for the CHO cell transfected with *mip-r1* (Fig. 7A and A' and Supplementary Fig. S1 C). The SGs have relatively high levels of the *mipr-1* transcript, with a Ct value of 24.8 in qRT-PCR (Fig. 4A). The complex interactions of the receptor's C-terminal end with other proteins could have masked the MIP-R1 epitope. Since this hypothetical phenomenon concealing the epitope could be cell (tissue)-specific, extended efforts may be required to develop a novel method for epitope retrieval in the SGs. Use of proteinase K digestion and heat for epitope retrieval has not been successful. Furthermore, the optical resolution that could be achieved for immunohistochemistry using confocal microscopy did not allow us to determine the exact cellular and subcellular locations of the SIFa-R-IR in the basal region of the acini, which is a complex structure containing multiple convoluted cells. Ultrastructural studies using transmission electron microscopy and immunogold staining will be required for further investigation.

MIPs are typically nine amino acids or slightly longer in length and exhibit the W(X6)Wamide motif; they are also known as type B allatostatins in *Gryllus bimaculatus* (Lorenz et al., 1995) or prothoracicostatic peptides (PTSP) in *Bombyx mori* (Hua et al., 1999). The MIPs exhibit a common functional activity in different species as inhibitors of gland and muscle activities (Davis et al., 2003; Kim et al., 2006; Lorenz et al., 1995; Schoofs et al., 1991). SIFamides, which are twelve amino acid-long peptides, are a group of highly conserved neuropeptides in different species of crustaceans and insects (Hauser et al., 2006; Yasuda et al., 2004) that exhibit stimulatory activity on the oviduct in *Locusta migratoria* (Janssen et al., 1996) and are involved in *Drosophila* sexual behavior (Terhzaz et al., 2007). In the control of tick SGs, these two peptides may exhibit opposing actions (i.e.,

NIH-PA Author Manuscript

NIH-PA Author Manuscript

NIH-PA Author Manuscript

inhibitory and stimulatory) on myoepithelial cells, basal dopaminergic cells, and/or neck cells. Unfortunately, RNA interference of the receptor genes mip-r1 and *sifa-r* was not successful for the suppression of their respective target transcripts in *I. scapularis* in our hands. Injections of the active peptides into the acinus, which is a challenging task because of a thick and strong basement membrane covering the acini, may reveal the physiological functions of the peptides in our on-going studies.

In addition to the receptors found in the SGs of *I. scapularis* in this study, transcripts for *mip-r* and *sifa-r* homologs have also been identified in the SGs of other tick species, including ES580804.1 as a *sifa-r* homolog in *Ornithodoros parkeri* and transcripts for both *sifa-r* and *mip-r* in *Amblyomma americanum,* as identified by Illumina sequencing (Park et al., unpublished data). Furthermore, our immunohistochemical analyses indicated the presence of peptidergic (i.e., MIP and SIFamide) innervation of the basal regions of the SGs in various tick species (Šimo et al., 2011a). Taken together, a mechanism using MIP and SIFamide, as well as their receptors, to control SG activity appears to be universally conserved in both hard and soft ticks.

Supplementary Material

Refer to Web version on PubMed Central for supplementary material.

Acknowledgments

We thank Dr. Richard Beeman and Joshua Urban for reviewing an earlier version of this manuscript. This paper is contribution no. 13–154-J from the Kansas Agricultural Experiment Station. The project described was supported by NIH Grant Numbers R01AI090062 and 1R21AI081136.

References

Binnington KC. Sequential changes in salivary gland structure during attachment and feeding of the cattle tick. *Boophilus microplus*. Int J Parasitol. 1978; 8:97–115. [PubMed: 681074]

Bowman AS, Coons LB, Needham GR, Sauer JR. Tick saliva: recent advances and implications for vector competence. Med Vet Entomol. 1997; 11:277–285. [PubMed: 9330260]

Bowman AS, Sauer JR. Tick salivary glands: function, physiology and future. Parasitology. 2004; 129(Suppl):S67–S81. [PubMed: 15938505]

Christie AE. Neuropeptide discovery in *Ixodoidea*: an in silico investigation using publicly accessible expressed sequence tags. Gen Comp Endocrinol. 2008; 157:174–185. [PubMed: 18495123]

Coons LB, Lessman CA, Ward MW, Berg RH, Lamoreaux WJ. Evidence of a myoepithelial cell in tick salivary glands. Int J Parasitol. 1994; 24:551–562. [PubMed: 8082985]

Coons LB, Roshdy MA. Fine structure of the salivary glands of unfed male *Dermacentor variabilis* (Say) (Ixodoidea: Ixodidae). J Parasitol. 1973; 59:900–912. [PubMed: 4744522]

Davis NT, Blackburn MB, Golubeva EG, Hildebrand JG. Localization of myoinhibitory peptide immunoreactivity in *Manduca sexta* and *Bombyx mori*, with indications that the peptide has a role in molting and ecdysis. J Exp Biol. 2003; 206(Pt 9):1449–1460. [PubMed: 12654884]

Fawcett, DW.; Binnington, K.; Voigt, WP. The cell biology of the ixodid tick salivary gland. In: Sauer, JR.; Hair, JA., editors. Morphology physiology and behavioral biology of ticks. Chichester: Ellis Horwood; 1986. p. 22-45.

Hauser F, Williamson M, Cazzamali G, Grimmelikhuijzen CJ. Identifying neuropeptide and protein hormone receptors in *Drosophila melanogaster* by exploiting genomic data. Brief Funct Genomic Proteomic. 2006; 4(4):321–330. [PubMed: 17202123]

Hill CA, Wikel SK. The *Ixodes scapularis* Genome Project: an opportunity for advancing tick research. Trends Parasitol. 2005; 21:151–153. [PubMed: 15780833]

NIH-PA Author Manuscript

NIH-PA Author Manuscript

NIH-PA Author Manuscript

Hua YJ, Tanaka Y, Nakamura K, Sakakibara M, Nagata S, Kataoka H. Identification of a prothoracicostatic peptide in the larval brain of the silkworm, *Bombyx mori*. J Biol Chem. 1999; 274:31169–31173. [PubMed: 10531308]

Hummel NA, Li AY, Witt CM. Serotonin-like immunoreactivity in the central nervous system of two ixodid tick species. Exp Appl Acarol. 2007; 43:265–278. [PubMed: 18040871]

Janssen I, Schoofs L, Spittaels K, Neven H, Vanden, Broeck J, Devreese B, Van Beeumen J, Shabanowitz J, Hunt DF, De Loof A. Isolation of NEB-LFamide, a novel myotropic neuropeptide from the grey fleshfly. Mol. Cell. Endocrinol. 1996; 117:157–165. [PubMed: 8737375]

Jorgensen LM, Hauser F, Cazzamali G, Williamson M, Grimmelikhuijzen CJ. Molecular identification of the first SIFamide receptor. Biochem Biophys Res Commun. 2006; 340:696–701. [PubMed: 16378592]

Kaufman WR. Actions of some transmitters and their antagonists on salivary secretion in a tick. Am J Physiol. 1978; 235:R76–R81. [PubMed: 677342]

Kaufman WR, Phillips JE. Ion and water balance in the Ixodid tick *Dermacentor andersoni*. I. Routes of ion and water excretion. Journal of Experimental Biology. 1973a:523–536. [PubMed: 4765348]

Kaufman WR, Phillips JE. Ion and water balance in the Ixodid tick *Dermacentor andersoni*. II. Mechanism and control of salivary secretion. Experimental Biology. 1973b; 58:537–547.

Kaufman WR, Sloley DB, Tatchell RJ, Zbitnew GL, Diefenbach TJ, Goldberg JI. Quantification and cellular localization of dopamine in the salivary gland of the ixodid tick *Amblyomma hebraeum*. Experimental & Applied Acarology. 1999; 23:251–256.

Kim YJ, Žitňan D, Cho KH, Schooley DA, Mizoguchi A, Adams ME. Central peptidergic ensembles associated with organization of an innate behavior. Proc Natl Acad Sci U S A. 2006; 103:14211–14216. [PubMed: 16968777]

Koči J, Šimo L, Park Y. Validation of internal reference genes for real-time quantitative PCR studies in the tick *Ixodes scapularis*. Journal of Medical Entomology. 2012 in press.

Krolak JM, Ownby CL, Sauer JR. Alveolar structure of salivary glands of the lone star tick, *Amblyomma americanum* (L.): unfed females. J Parasitol. 1982; 68:61–82. [PubMed: 7200514]

Kumar S, Dudley J, Nei M, Tamura K. MEGA: a biologist-centric software for evolutionary analysis of DNA and protein sequences. Brief Bioinform. 2008; 9:299–306. [PubMed: 18417537]

Livak KJ, Schmittgen TD. Analysis of relative gene expression data using real-time quantitative PCR and the 2(-Delta Delta C(T)) Method. Methods. 2001; 25:402–408. [PubMed: 11846609]

Lorenz MW, Kellner R, Hoffmann KH. Identification of two allatostatins from the cricket, *Gryllus bimaculatus* de Geer (Ensifera, Gryllidae): additional members of a family of neuropeptides inhibiting juvenile hormone biosynthesis. Regul Pept. 1995; 57:227–236. [PubMed: 7480872]

McSwain JL, Essenberg RC, Sauer JR. Oral secretion elicited by effectors of signal transduction pathways in the salivary glands of *Amblyomma americanum* (Acari: Ixodidae). J Med Entomol. 1992; 29:41–48. [PubMed: 1552527]

Meredith J, Kaufman WR. A proposed site of fluid secretion in the salivary gland of the ixodid tick Dermacentor andersoni. Parasitology. 1973; 67:205–217. [PubMed: 4127146]

Neupert S, Russell WK, Predel R, Russell DH, Strey OF, Teel PD, Nachman RJ. The neuropeptidomics of *Ixodes scapularis* synganglion. J Proteomics. 2009; 72:1040–1045. [PubMed: 19540946]

Park, Y.; Adams, ME. Insect G protein-coupled receptors. In: Gilbert, LI.; Iatrou, K.; Gill, SS., editors. Insect Pharmacology. London: Academic Press; 2010. p. 330-362.

Park Y, Kim YJ, Adams ME. Identification of G protein-coupled receptors for *Drosophila* PRXamide peptides, CCAP, corazonin, and AKH supports a theory of ligand-receptor coevolution. Proc Natl Acad Sci U S A. 2002; 99:11423–11428. [PubMed: 12177421]

Park Y, Kim YJ, Dupriez V, Adams ME. Two subtypes of ecdysis-triggering hormone receptor in *Drosophila melanogaster*. J Biol Chem. 2003; 278:17710–17715. [PubMed: 12586820]

Ribeiro JM, Alarcon-Chaidez F, Francischetti IM, Mans BJ, Mather TN, Valenzuela JG, Wikel SK. An annotated catalog of salivary gland transcripts from *Ixodes scapularis* ticks. Insect Biochem Mol Biol. 2006; 36:111–129. [PubMed: 16431279]

NIH-PA Author Manuscript

NIH-PA Author Manuscript

NIH-PA Author Manuscript

Roshdy MA, Coons LB. The subgenus Persicargas (Ixodoidea: Argasidae: Argas). 23. Fine structure of the salivary glands of unfed A. (P.) arboreus Kaiser, Hoogstraal, and Kohls. J Parasitol. 1975; 61:743–752. [PubMed: 1165559]

Sauer JR, Hair JA. Water balance in the lone star Tick (Acarina: Ixodidae): the effects of relative humidity and temperature on weight changes and total water content. Journal of Medical Entomology. 1971; 8:479–485. [PubMed: 5160247]

Sauer JR, McSwain JL, Bowman AS, Essenberg RC. Tick salivary gland physiology. Annu Rev Entomol. 1995; 40:245–267. [PubMed: 7810988]

Schoofs L, Holman GM, Hayes TK, Nachman RJ, De Loof A. Isolation, identification and synthesis of locustamyoinhibiting peptide (LOM-MIP), a novel biologically active neuropeptide from *Locusta migratoria*. Regul Pept. 1991; 36(1):111–119. [PubMed: 1796179]

Šimo L, Koči J, Žitňan D, Park Y. Evidence for D1 dopamine receptor activation by a paracrine signal of dopamine in tick salivary glands. PLoS One. 2011a; 6:e16158. [PubMed: 21297964]

Šimo L, Slovák M, Park Y, Žitňan D. Identification of a complex peptidergic neuroendocrine network in the hard tick, *Rhipicephalus appendiculatus*. Cell Tissue Res. 2009a; 335:639–655. [PubMed: 19082627]

Šimo L, Žitňan D, Park Y. Two novel neuropeptides in innervation of the salivary glands of the black-legged tick, *Ixodes scapularis*: myoinhibitory peptide and SIFamide. J Comp Neurol. 2009b; 517:551–563. [PubMed: 19824085]

Šimo L, Žitňan D, Park Y. Neural control of salivary glands in ixodid ticks. J Insect Physiol. 2011b; 58:459–466. [PubMed: 22119563]

Sonenshine, DE. Biology of ticks. Vol. vol 1. Oxford: Oxford University Press; 1991.

Terhzaz S, Rosay P, Goodwin SF, Veenstra JA. The neuropeptide SIFamide modulates sexual behavior in *Drosophila*. Biochem Biophys Res Commun. 2007; 352:305–310. [PubMed: 17126293]

Thompson JD, Higgins DG, Gibson TJ. CLUSTAL W: improving the sensitivity of progressive multiple sequence alignment through sequence weighting, position-specific gap penalties and weight matrix choice. Nucleic Acids Res. 1994; 22:4673–4680. [PubMed: 7984417]

Tusnady GE, Simon I. Principles governing amino acid composition of integral membrane proteins: application to topology prediction. J Mol Biol. 1998; 283:489–506. [PubMed: 9769220]

Vernon WI, Printen JA. Assay for intracellular calcium using a codon-optimized aequorin. Biotechniques. 2002; 33:730–734. [PubMed: 12398176]

Yapici N, Kim YJ, Ribeiro C, Dickson BJ. A receptor that mediates the post-mating switch in *Drosophila* reproductive behaviour. Nature. 2008; 451:33–37. [PubMed: 18066048]

Yasuda A, Yasuda-Kamatani Y, Nozaki M, Nakajima T. Identification of GYRKPPFNGSIFamide (crustacean-SIFamide) in the crayfish *Procambarus clarkii* by topological mass spectrometry analysis. Gen Comp Endocrinol. 2004; 135:391–400. [PubMed: 14723891]

NIH-PA Author Manuscript

NIH-PA Author Manuscript

NIH-PA Author Manuscript

- Receptors for two neuropeptides, MIP and SIFamide, were identified and characterized in the tick salivary glands.
- Immunohistochemistry of SIFamide receptor revealed three candidate target cells of the SIFamide.
- The target cells of the SIFamide are proposed to be myoepithelial cell, basal granular cell, and neck cells.

NIH-PA Author Manuscript
NIH-PA Author Manuscript
NIH-PA Author Manuscript

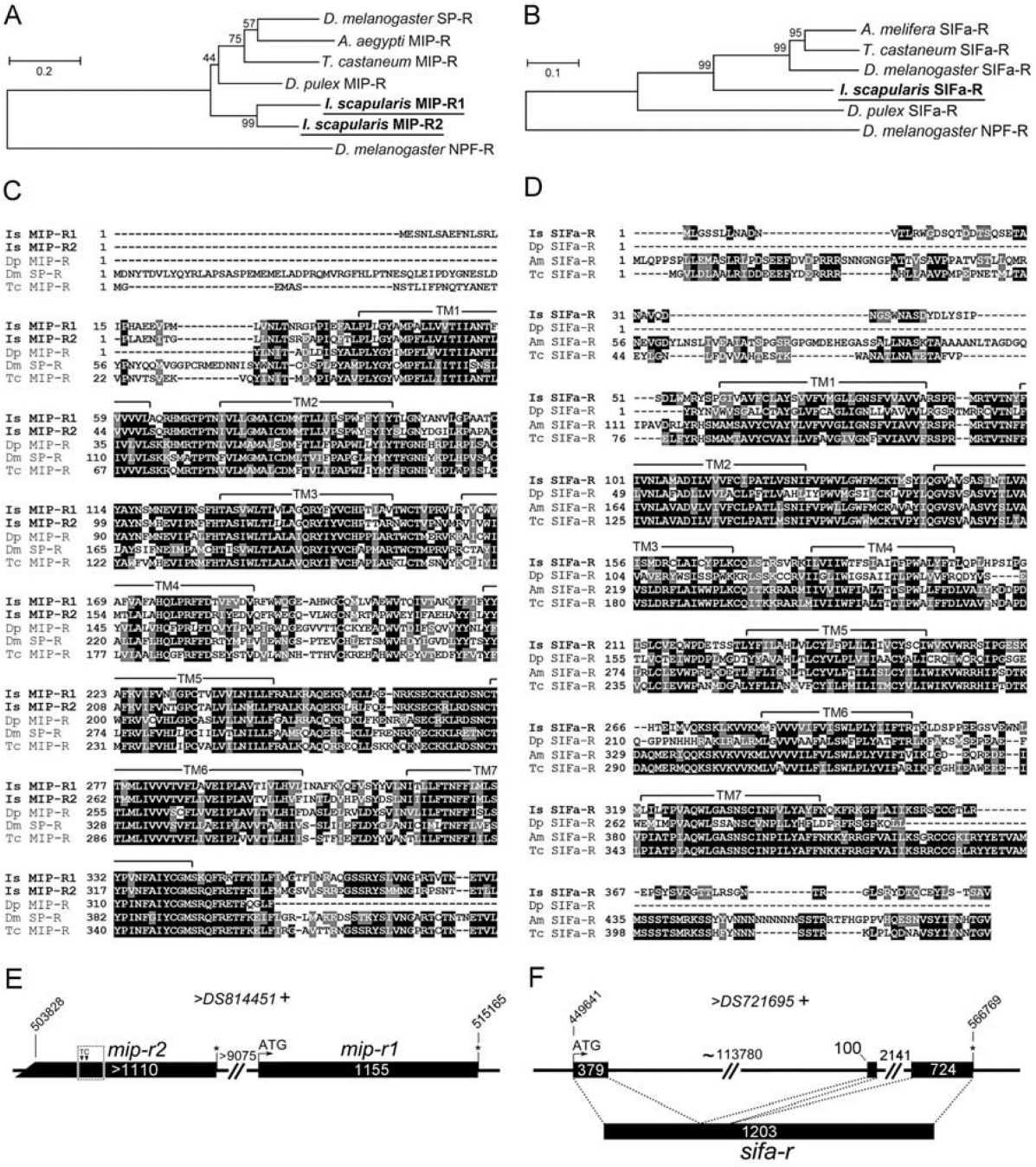

Figure 1.

Phylogenetic analyses and open reading frames (ORF) for the *I. scapularis* myoinhibitory peptide receptors (MIP-R) and SIFamide receptor (SIFa-R). (A) The phylogenetic relationship of MIP-Rs of various arthropod species, including two MIP-Rs from *I. scapularis*. (B) The phylogenetic relationship of SIFa-Rs of different arthropod species. The trees were constructed using a neighbor-joining method. The number at each node indicates the percent support from 500 bootstrap replicates. The *Drosophila* neuropeptide F receptor (NPF-R) sequence was used as the out-group for both analyses. (C, D) Alignments of predicted translations of the two *Ixodes* MIP receptors (C) and one SIFamide receptor (D) with other related sequences. The letters highlighted by a gray background are similar and

NIH-PA Author Manuscript

NIH-PA Author Manuscript

NIH-PA Author Manuscript

the letters highlighted by a black background are identical amino acids in a 50% majority rule. Conserved seven-transmembrane segments (TM1–7) were predicted using the HMMTOP Server v2.0 software (http://www.enzim.hu/hmmtop/) and are indicated by a solid line above the alignment. (E) *mip-r1* and *mip-r2* are intronless and tandemly repeated in the same scaffold. Note that *mip-r2* is incomplete at its 5' end and is thus considered to be a pseudogene. Two nucleotide insertions (a T and a C) found in our experiment (dotted box) compared to the *I. scapularis* genomic data are marked (see Supplemental Fig.S2 B). (F) The ORF of *sifa-r* contains three exons. The numbers in each box and on the lines represent the lengths (bp) of the exons and introns, respectively. The italicized numbers are the coordinates of the gene in the scaffold. The plus sign (+) after the scaffold name indicates the forward direction. Putative translation initiation sites and stop codons are marked by an ATG and an asterisk (*), respectively. The GenBank Accession numbers are as follows: *D. melanogaster* SP-R, AAF46037.2; Aedes aegypti MIP-R, ABW86944.1; *T. castaneum* MIP-R, NP_001106940.1; *Daphnia pulex* MIP-R, EFX82580.1; *I. scapularis* MIP-R1, KC422390, and MIP-R2, KC422391; *D. melanogaster* NPF-R, AF364400.1; *Apis melifera* SIFa-R, NP_001106756.1; *T. castaneum* SIFa-R, XP_970225.1; *D. melanogaster* SIFa-R, NP_650966.2; *I. scapularis* SIFa-R, KC422392; and *D. pulex* SIFa-R, EFX84166.1.

NIH-PA Author Manuscript
NIH-PA Author Manuscript
NIH-PA Author Manuscript

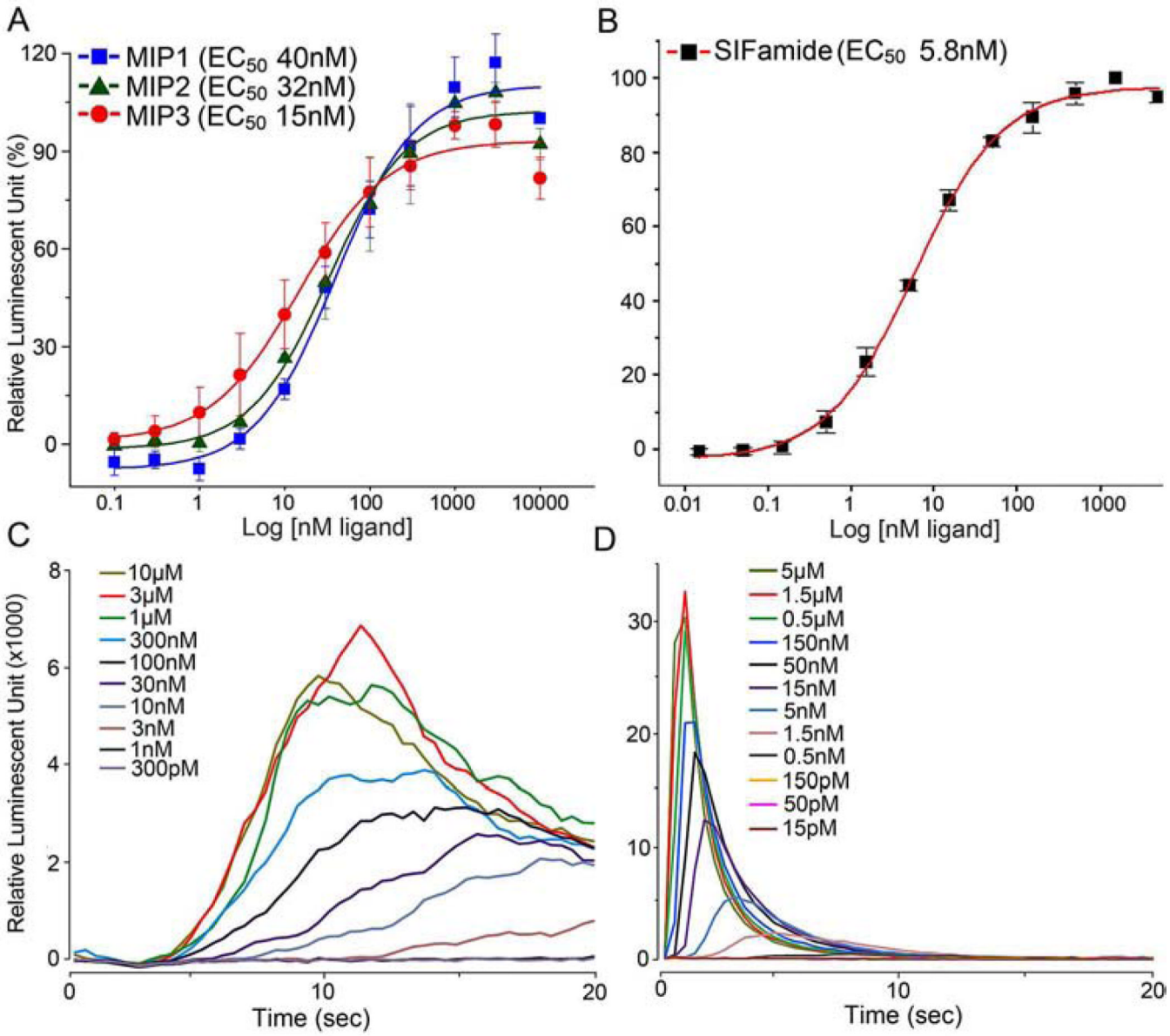

Figure 2.

Aequorin reporter assays in CHO cells that were transfected with either myoinhibitory peptide receptor (MIP-R1; A, C) or SIFamide receptor (B, D). The results are the cellular responses observed after ligand-mediated calcium mobilization. (A) The dose-response curves for MIP-R1 to the MIP ligands (i.e., MIPs 1, 2, and 3) in *I. scapularis*. (B) The dose-response curve for SIFa-R to *I. scapularis* SIFamide. (C) Representative responses of the cells to MIP-R1 when treated with different doses of the MIP ligands (MIP2 in this case). (D) Representative responses of the cells to SIFa-R when treated with different doses of SIFamide. The bars in A and B indicate the standard error for a minimum of three replicates.

NIH-PA Author Manuscript

NIH-PA Author Manuscript

NIH-PA Author Manuscript

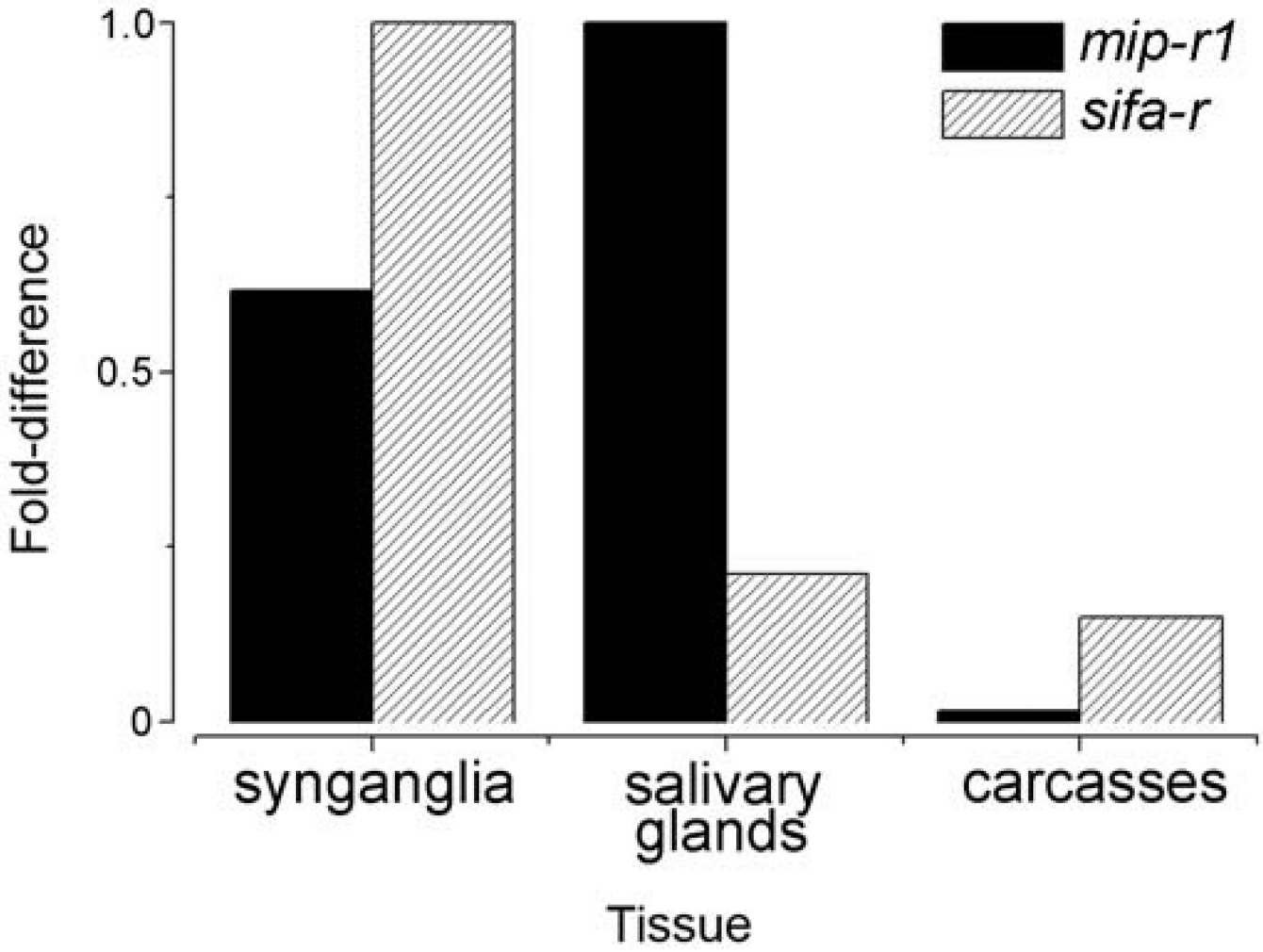

Figure 3.
mRNA levels of myoinhibitory peptide receptor 1 (MIP-R1) and SIFamide receptor (SIFa-R) as measured by qRT-PCR analyses in different tissues. Note that the cDNAs used were from pools of tissues from daily collections of unfed, 1–6 day fed, and fully engorged females. The data were normalized to the ribosomal protein S4 (RPS4) transcript control, and the highest expression levels were assigned a value of 1.

NIH-PA Author Manuscript
NIH-PA Author Manuscript
NIH-PA Author Manuscript

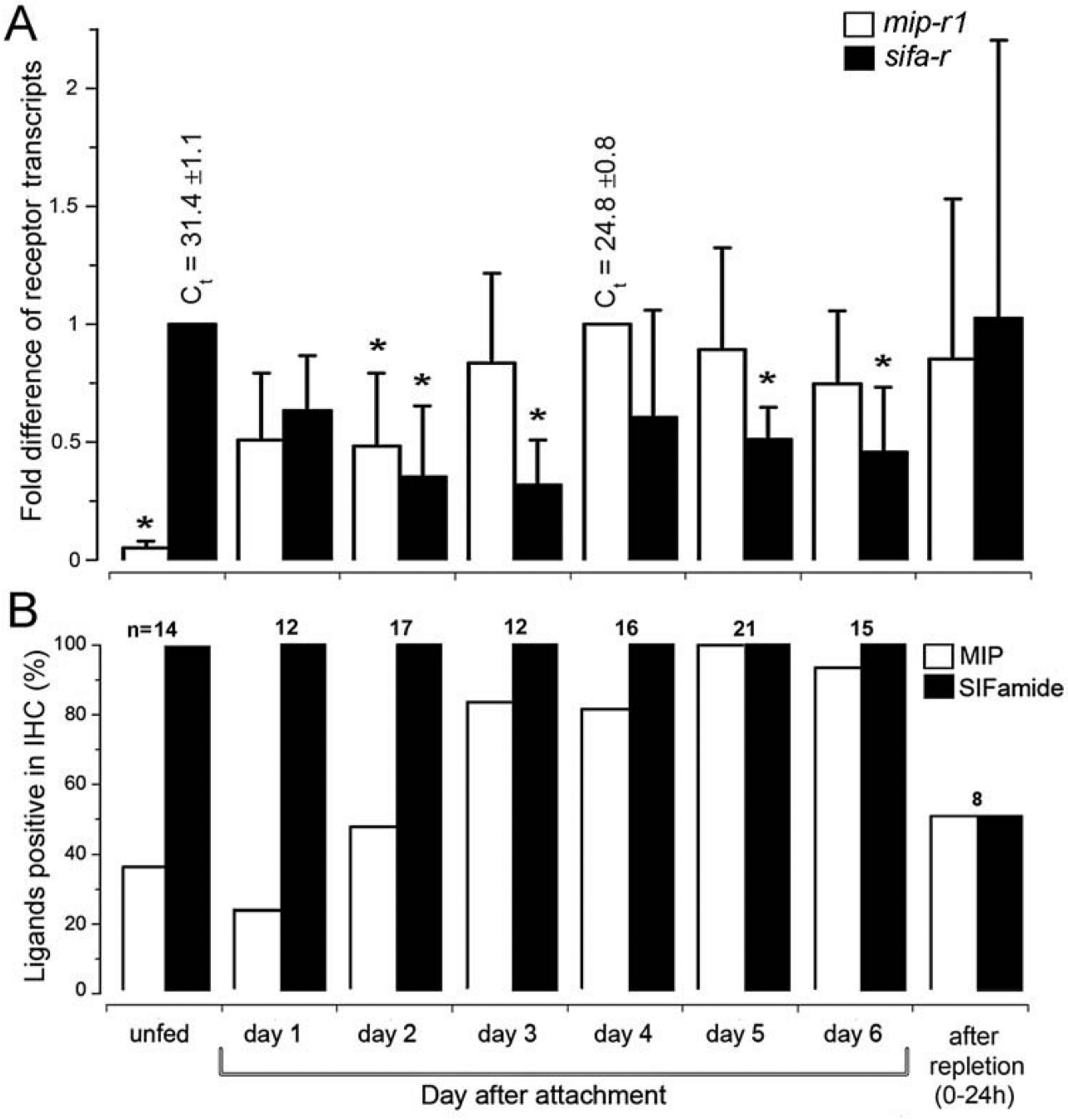

Figure 4.

Changes in the mRNA levels of myoinhibitory peptide receptor 1 (MIP-R1) and SIFamide receptor (SIFa-R) and the immunohistochemical reactions of the ligands in the salivary glands during various feeding phases. (A) Levels of the receptor transcripts, *mip-r1* and *sifa-r*, in the salivary glands. (B) Immunohistochemical analysis of the frequency of positive individual females for the MIP and SIFamide neuropeptides in the salivary gland regions that contain the basal axon terminals. The bars in panel A indicate the standard deviation for a minimum of four biological replicates. The asterisk (*) indicates the comparison of the mean to the highest value using a one-way Student t-test ($P \leq 0.05$). The data were normalized using the ribosomal protein S4 (RPS4) transcript, and the highest expression

levels were assigned a value of 1; the Ct values (i.e., the mean ± standard deviation) for the biological replicates are shown. The numbers above the bars in panel B indicate the number of salivary glands used for each data point. Further experimental details can be found in the section 2.4 Quantitative real-time reverse transcriptase-PCR (qRT-PCR).

NIH-PA Author Manuscript
NIH-PA Author Manuscript
NIH-PA Author Manuscript

NIH-PA Author Manuscript
NIH-PA Author Manuscript
NIH-PA Author Manuscript

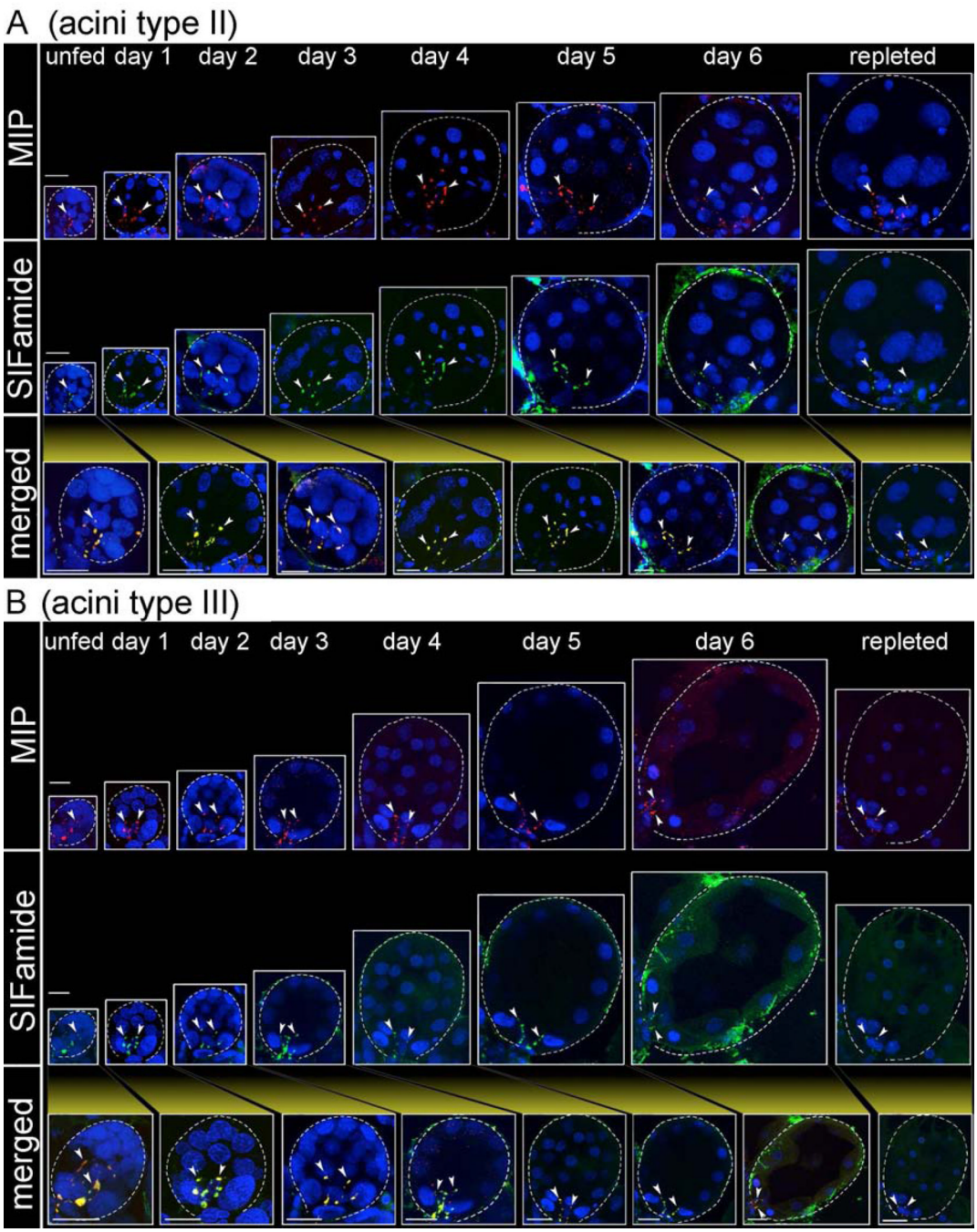

Figure 5.

Immunoreactivity observed in the axon terminals within type II (A) and type III (B) acini for myoinhibitory peptide (MIP, red) and SIFamide (green in); merged images are shown in yellow. Salivary gland acini types II and III are from salivary glands collected daily from unfed to fully engorged females (repleted), which is indicated by their proportional sizes. Note that immunoreactive axon terminals (arrow heads) are associated exclusively with the basal regions of acini types II and III. For frequency of positively stained individuals, see Fig. 4B. Dotted lines indicate the boundary of an acinus. Cell nuclei were stained with DAPI (blue). The scale bars indicate 20 μm.

NIH-PA Author Manuscript
NIH-PA Author Manuscript
NIH-PA Author Manuscript

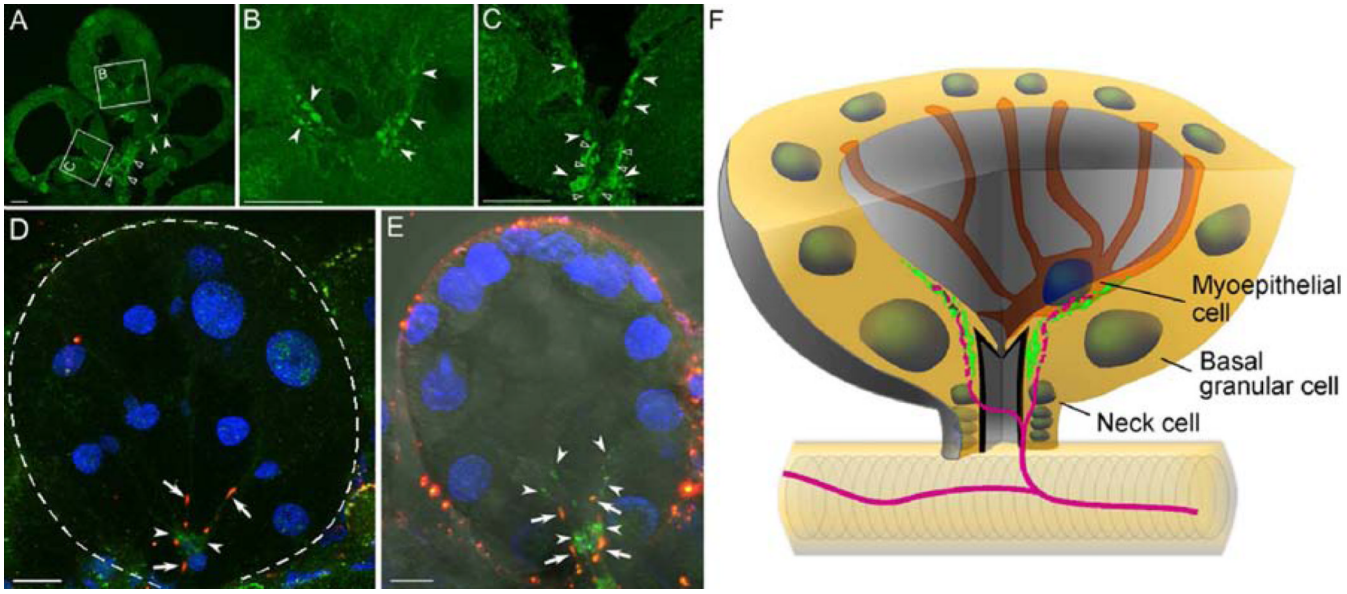

Figure 6.

Immunohistochemical analysis of the SIFamide receptor (SIFa-R, green, arrowhead) in tick salivary glands. (A, B, C) Type III acini were isolated from four-day-fed females and sectioned. The empty arrow heads indicate the salivary duct in A and the acinar duct in C, which were obscured by the autofluorescence of the cuticular lining of the duct. (D, E) The SIFamide neuropeptide (red, arrow) and its receptor (SIFa-R, green, arrow head) in a whole-mount staining of acini type II (D, 5-day-fed female) and acini type III (E, 4-day-fed female). Note that the neuropeptidergic signal (red) is closely associated with the basally localized SIFa-R (green). Fluorescence surrounding the acinus is non-specific noise, often associated with Bouin's fixation. (F) Simplified diagram of the acini type III basal region. The nuclei of different cells are shown as round circles. SIFamide peptidergic innervations (magenta) are closely associated with SIFa-R receptors (green) as depicted. Three different types of cells in the basal region are annotated, with the cell boundary indicated only for the mypepithelial cell, as described in (Krolak et al., 1982). The dotted line in D indicates the boundary of an acinus. The scale bar indicates 10 μm.

NIH-PA Author Manuscript
NIH-PA Author Manuscript
NIH-PA Author Manuscript

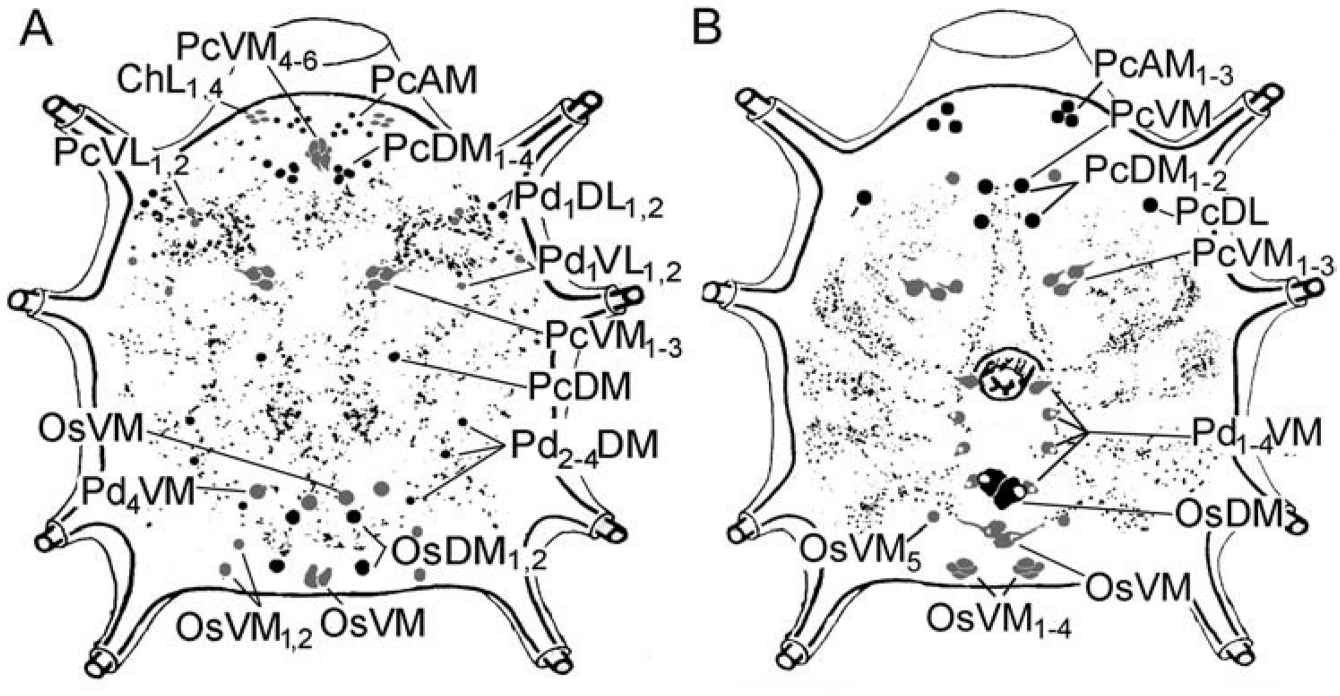

Figure 7.

Schematic diagram of the synganglia showing all the neurons and their projections, as well as their reaction to antibodies for myoinhibitory peptide receptor 1 (MIP-R1, five-day-fed females, A) and SIFamide receptor (SIFa-R, four-day-fed females, B). Black indicates dorsal neurons, and gray indicates ventral neurons. An explanation of the abbreviations of the labeled neurons is provided in section 2.6 The nomenclature of peptidergic neurons and in Šimo et al. (2009a).

NIH-PA Author Manuscript
NIH-PA Author Manuscript
NIH-PA Author Manuscript

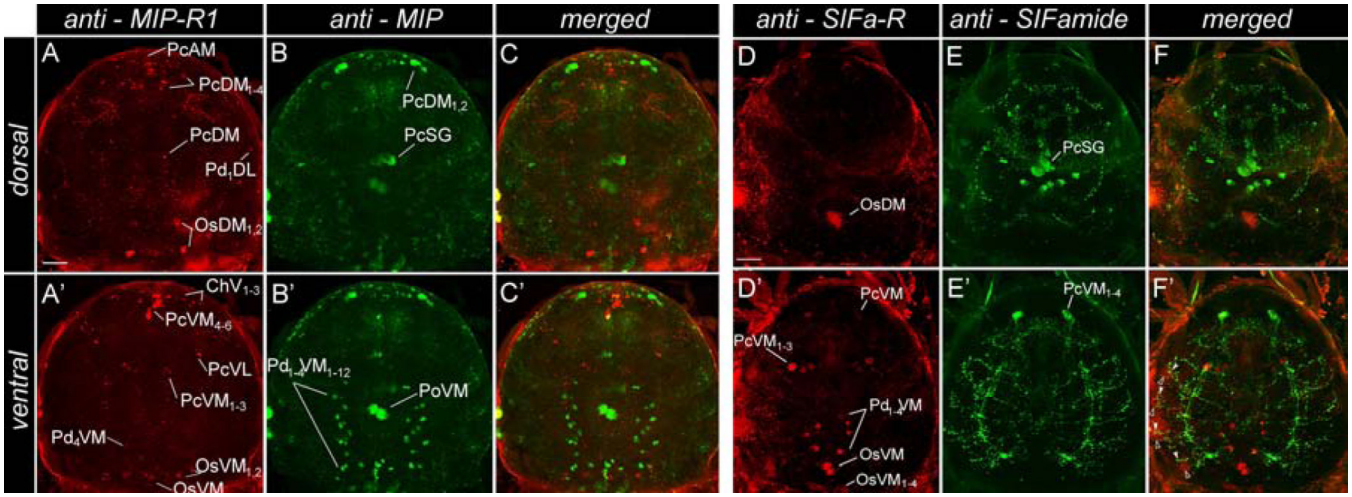

Figure 8.

Immunohistochemistry showing the double staining of neurons producing neuropeptides and their receptors in the tick synganglion. (A and A') anti-myoinhibitory peptide receptor 1 (MIP-R1, red) and (B and B') anti-MIP (MIP, green) in 5-day-fed female; the respective merged images are shown in C and C'. (D and D') anti-SIFamide receptor (SIFa-R, red) and (E and E') anti-SIFamide (SIFamide, green) in 5-day-fed female; the respective merged images are shown in F and F'. Note that the segmental, SIFamide-positive projections in pedal lobes I–IV (green, arrow head) are closely associated with the SIFa-R-positive projection in F' (red, empty arrow head). The upper panel (A to F) shows the dorsal side of a synganglion, while the lower panel (A' to F') shows the ventral side. Abbreviations of the labeled neurons are explained in section 2.6 The nomenclature of peptidergic neurons and in Šimo et al. (2009a). The bright edges of the synganglion are due to autofluorescence. The scale bar indicates 50 μm.

NIH-PA Author Manuscript
NIH-PA Author Manuscript
NIH-PA Author Manuscript

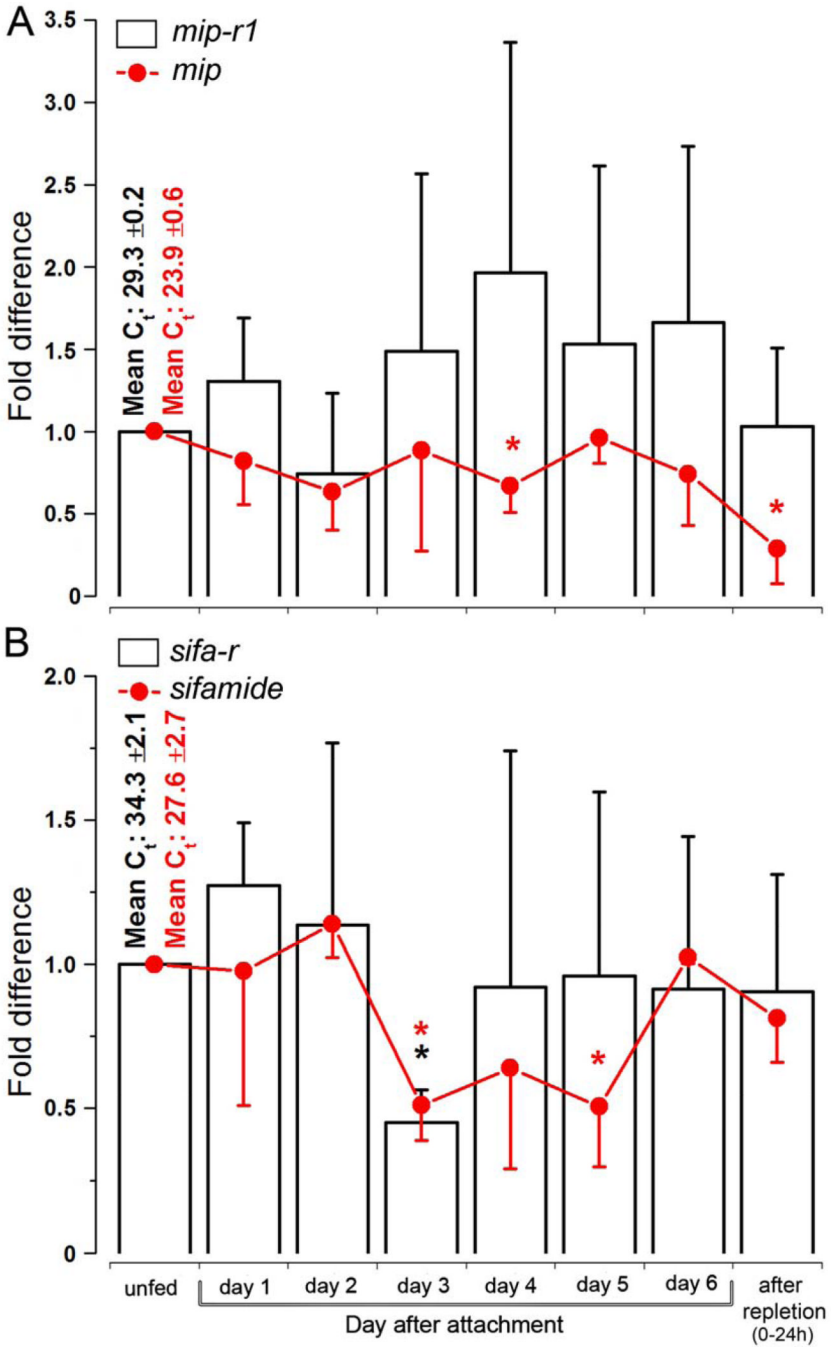

Figure 9.

The transcript levels of myoinhibitory peptide (*mip*) and *sifamide* and their receptors, *mip-r1* and *sifa-r*, in synganglia over the course of feeding. (A) The transcript levels of *mip* (red line) and *mip-r1* (black bars) in synganglia. (B) The transcript levels of *sifamide* (red lines) and *sifa-r* (black bars) in synganglia. The bars indicate the standard deviation for a minimum of four biological replicates. The asterisk (*) indicates the comparison of the mean to the highest value using a one-way Student t-test ($P \leq 0.05$). The data were normalized using ribosomal protein S4 (RPS4), and the highest expression levels were considered to be a value of 1; the Ct values (i.e., the mean ± standard deviation) for the biological replicates are shown.

NIH-PA Author Manuscript

NIH-PA Author Manuscript

NIH-PA Author Manuscript

Table 1

Primers used for gene cloning and qPCR in this study. The underlined CACC sequence at the 5’ end of the *mip-r1* forward primer was for the directional cloning of the gene into the expression vector.

Name	Forward primer (5’-3’)	Reverse primer (5’-3’)
Primers for ORF		
mip-r1	CACCATGGAAAGCAACCTTTC	TTAGAGAACAGTTTCATTTG
sifa-r	ACCATAGCGAACGTCAAGAGAC	AGTTACACAGCCGACGTGGAGA
Primers for qRT-PCR		
mip-r1	AGGTGCCGATGCTGGTCAA	GATGTAGAAGAACCAAGGC
mip	GACTGGAACGCGCTGTCAGGC	TGTGTCGAAGCCGCGCGCTTCC
sif-r	ACACGTCCCAGTCAGAGA	AAACACCACCGAGTAGGC
sifa	TATGTTTGGCACGCTTTTGG	CCAGACAGCTTCACACATTG
rpS4	GGTGAAGAAGATTGTCAAGCAGAG	TGAAGCCAGCAGGGTAGTTTG